

# Design and Analysis of a Large-Span Spiral Spatial Antisymmetric Ribbon Landscape Arch Bridge

Xiaozhu Teng

Tongji Architectural Design (Group) Co., Ltd., Shanghai 200092, China.  
Correspondence: bamboo389@126.com

**Abstract:** The Xiaohe River Bridge on Dayun Road is the world's first large-span spiral-shaped spatially asymmetric landscape arch bridge. This bridge breaks through the traditional arch bridge design, refining the curve elements and transforming them into a closed spiral-shaped spatial ribbon arch bridge comprising two spans of asymmetric ribbon inclined secondary arches and a single span of a diagonal main arch. This design creates a sense of passage and dynamic movement, with nested arches and landscapes. The bridge has a total span arrangement of  $65+110+110+65 = 350$  m. The main beam and transverse beams are connected with the main and secondary arches, forming an arch-beam joint system. This structure transforms the mechanical properties of the irregular spiral-shaped spatially asymmetric ribbon landscape arch bridge into an arch-beam composite system. This system is characterized by structural self-balancing and no horizontal thrusts. The main and secondary arch ribs are designed with parabolic arch axes and box-type cross sections. The main arch span is 229 m, which is the largest diagonal spanning arch bridge in China. The transition segments (the arch feet) connecting the main and secondary arches with the transverse beams are twisted surface components made from Q370qD steel with a plate thickness of 40 mm. The main beam adopts a semi-closed double-sided steel box section. The bridge has undergone comprehensive analyses, including spatial static, fatigue, stability, and seismic performance evaluations, as well as refined analysis of the arch feet. The results indicate that the structure is safe, reliable, and meets the relevant design code requirements.

**Keywords:** landscape arch bridge, spatial antisymmetric ribbon arch, diagonal main arch, outward-inclined secondary arch, arch-beam combination system

**Citation:** Teng, X. Design and Analysis of a Large-Span Spiral Spatial Antisymmetric Ribbon Landscape Arch Bridge. *Prestress Technology* 2024, 4, 83-95.  
<https://doi.org/10.59238/j.pt.2024.04.006>

Received: 18/11/2024

Accepted: 24/12/2024

Published: 30/12/2024

**Publisher's Note:** Prestress technology stays neutral with regard to jurisdictional claims in published maps and institutional affiliations.



**Copyright:** © 2024 by the authors. Submitted for possible open access publication under the terms and conditions of the Creative Commons Attribution (CC BY) license (<https://creativecommons.org/licenses/by/4.0/>).

## 1 Project Overview

The Xiaohe River Bridge is located on Dayun Road in the Comprehensive Reform Demonstration Zone of Taiyuan, Shanxi Province. It spans the Xiaohe River and forms a semi-interchange overpass with Xiaohe South Road and Xiaohe North Road. The main line is 1,164 m long in total, with the bridge section being 968 m long. The bridge is located in the core area of the Xiaohe River scenic landscape, not only serving as a crucial transportation link for north-south traffic but also acting as an important scenic landmark.

The bridge is located in the southern part of the Taiyuan Basin, within a moderately stable engineering geological subzone. The site contains a layer of fine sand and silty sand, which poses challenges for structural seismic performance and pile foundation construction. The main technical standards for the bridge are as follows:

- Road Classification: Urban arterial road with a right-of-way width of 66 m and a design speed of 60 km/h.
- Design Load: Class A for urban roads.
- Design Safety Level: Class I, with a design reference period and service life both set at 100 years.
- Seismic Design Standards: Basic seismic intensity of degree 8, with peak accelerations for earthquakes with return periods of 475 years and 2475 years of 0.221g and 0.426g, respectively. The characteristic period of the design is 0.55 s, and the seismic protection category for the main bridge is Category B.
- Wind Resistance Design Standards: The basic design wind speed is 32.6 m/s.

- Hydrological and Navigation Standards: The design flood level for a 100-year return period is 776.4 m, with the normal water level at 773.5 m. The bridge does not have specific navigation requirements.

## 2 Bridge Form and Overall Design

### 2.1 Bridge Form Design



**Figure 1** Landscape view of the Xiaohe River Bridge

The Xiaohe River Bridge incorporates design elements such as "mountains, water, people, and culture," extracting curve elements inspired by the local landscape and cultural characteristics. In combination with the surrounding environmental and scenic requirements, it uniquely features a spiral-shaped spatial antisymmetric ribbon arch bridge, which is an original creation in bridge architecture. The design of the bridge is world first. The bridge breaks through traditional arch bridge forms, with the main arch oriented diagonally across two main spans, whereas the inclined secondary arches are located on both sides of the main span. The arches are connected by transverse beams, creating a closed, spiral-shaped, antisymmetric ribbon landscape arch. This design creates a sense of passage and dynamic movement, with arches within arches and landscapes within landscapes [1]. The spiral-shaped, antisymmetric ribbon arch structure is rich in spatial complexity, employing the golden ratio for harmonious and aesthetically pleasing proportions. From all viewing angles, the bridge displays a unique variation in shape. Wandering between the graceful, floating arch ribs, one feels immersed in the shifting landscapes of the Shanxi region (see Figure 1). The arch, beams, and cables are pure white (metallic color), reflecting a design philosophy of purity, nature, ecology, and technology.

### 2.2 Overall Design and Structural System

The main and approach bridges of the Xiaohe River Bridge are located along a straight section of Dayun Road, with the bridge elevation situated on a vertical curve with a radius of 6000 m. The maximum longitudinal slope of the main bridge is 1.5%, whereas the maximum longitudinal slope of the southern and northern approach bridges is 3.49%. The bridge is located in an area where the planned width of the Xiaohe River is approximately 500 m. Considering flood control and landscape requirements, the main bridge span is arranged as  $65 + 110 + 110 + 65 = 350$  m (see Figure 2). The main bridge width is 46 m, with a functional width of 44.5 m, providing eight lanes for bidirectional traffic. The deck layout is as follows: 2.5 m (sidewalk) + 4 m (nonmotorized vehicle lane) + 0.5 m (collision barrier) + 15 m (motor vehicle lane) + 0.5 m (central collision barrier) + 15 m (motor vehicle lane) + 0.5 m (collision barrier) + 4 m (nonmotorized vehicle lane) + 2.5 m (sidewalk) = 44.5 m. The bridge arch ribs are designed with a rectangular steel box section, whereas the main beams

are made of semi-closed double-sided steel box sections. The substructure comprises pier caps and a pile foundation.

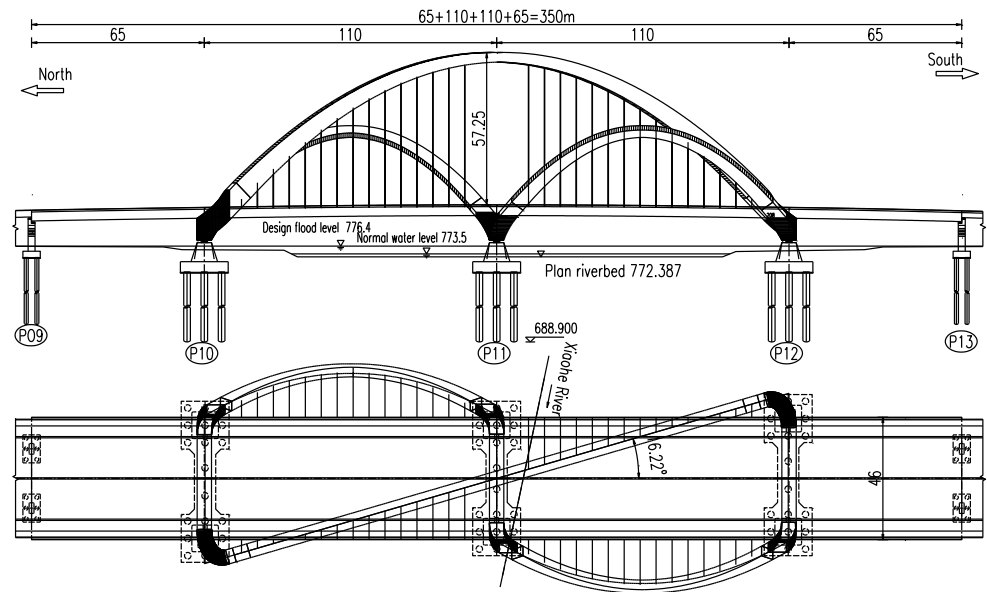


**Figure 2** Overall layout of the main bridge of the Xiaohe River Bridge (Unit: m)

The bridge arch ribs consist of a single diagonal main arch and two outward-inclined secondary arches on either side, forming an antisymmetric shape. The main arch spans 229 m, and after crossing the two main spans, it connects with the outward-inclined secondary arches through transverse beams. The secondary arches are inclined at an angle of 25° and are located on the east and west sides of the main span. At the middle support point, they are connected by transverse beams, and at the end support points of the main span, they connect with the main arch via transverse beams. Under the action of cables, there is a tendency for clockwise torsion (see Figure 3).

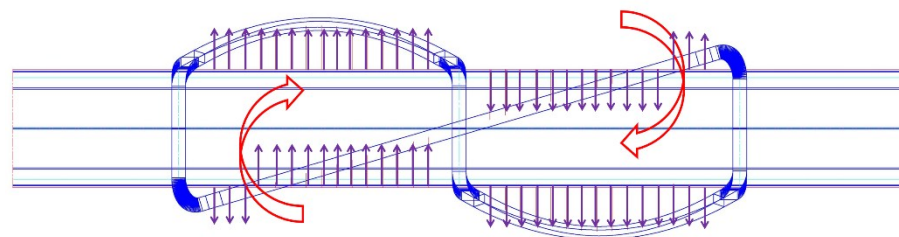


**Figure 3** Deformation trend of the main beam

For the site located in a seismic zone with a seismic intensity of 8 degrees, three design schemes were considered: arch–pier–beam consolidation, arch–pier consolidation (see Figure 4), and arch–beam consolidation (see Figure 5). The first two systems result in excessive longitudinal horizontal thrust, leading to large foundation sizes and high costs. In the arch–pier consolidation system, the main beam experienced considerable lateral horizontal thrust. The arch–beam consolidation system connects the main beam with the spatial bending–twisting surface arch feet of the main and secondary arches through transverse beams. After the arch–beam connection, seismic bearings are installed beneath the transverse beams. These measures transform the complex spatially antisymmetric ribbon–arch bridge into a more straightforward tied arch bridge with clear load paths. The main girder and the transverse beams act as tie rods, counteracting the horizontal thrust generated by the arch ribs. To address the plane torsion issue caused by the antisymmetric horizontal forces from the antisymmetric arch cables, the plane stiffness of the main beam is used to

achieve a balance. The horizontal thrusts of the entire bridge, both longitudinal and diagonal from the arch ribs, are primarily borne by the box girder, and the complex load distribution is largely balanced within the arch–beam system. The maximum horizontal force generated by the horizontal fixed supports is 6.5% of the vertical force at the side arch foot and 10.6% at the central arch foot, thereby reducing the size of the bearings and the foundation scale.

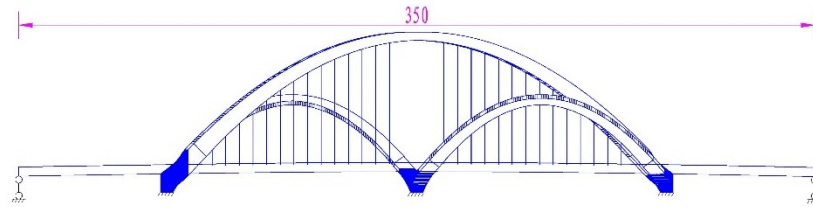


**Figure 4** Arch–pier–beam consolidation and arch–pier consolidation elevation (Unit: m)

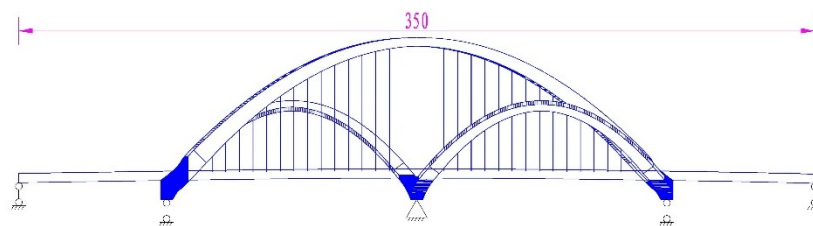


**Figure 5** Arch–beam consolidation elevation (Unit: m)

### 3 Bridge Structural Design

#### 3.1 Arch Ribs [2]

The main bridge's antisymmetric ribbon arch ribs comprise a large main arch with a diagonal crossing two main spans, two outward–inclined secondary arches distributed on both sides of the main span, and their connecting transverse beams. All the arch ribs adopt a parabolic arch axis line and have a rectangular steel box cross section.

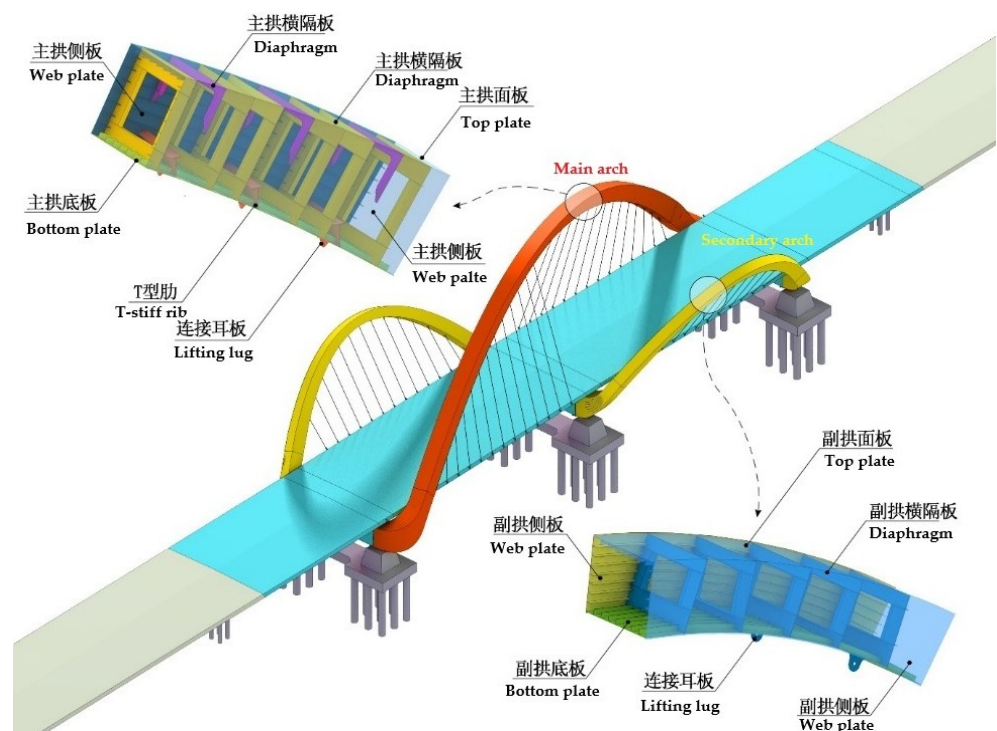


**Figure 6** Perspective diagram of the main bridge arch ribs

### 3.1.1 Main Arch

The main arch spans diagonally from the southeast side of the main bridge to the northwest side. At the side arch feet, the main arch connects to the secondary arch through a transverse beam beneath the main beam. The plane of the main arch ribs is vertical, with an angle of  $16.22^\circ$  between the main arch plane and the longitudinal axis of the bridge. The main arch span is 229.12 m, with a distance of 57.25 m from the arch crown to the bridge deck. The main segment of the arch axis is a parabola, with a rise of 56.5 m and a span of 225 m, resulting in a rise-to-span ratio of 1/4. The connection between the arch feet and the transverse beam uses a circular arc with a radius of 10.5 m. A straight-line transition is used between the parabolic and circular arc segments. The cross section of the main arch ribs is rectangular. The parabolic segment of the arch ribs has a variable cross section (see Figure 7), with dimensions of  $B \times H = 5.5 \text{ m} \times 8.1 \text{ m}$ , where it transitions to the straight segment, and dimensions of  $B \times H = 5.5 \text{ m} \times 3.6 \text{ m}$  at the vertex of the parabola, with linear variation in between.

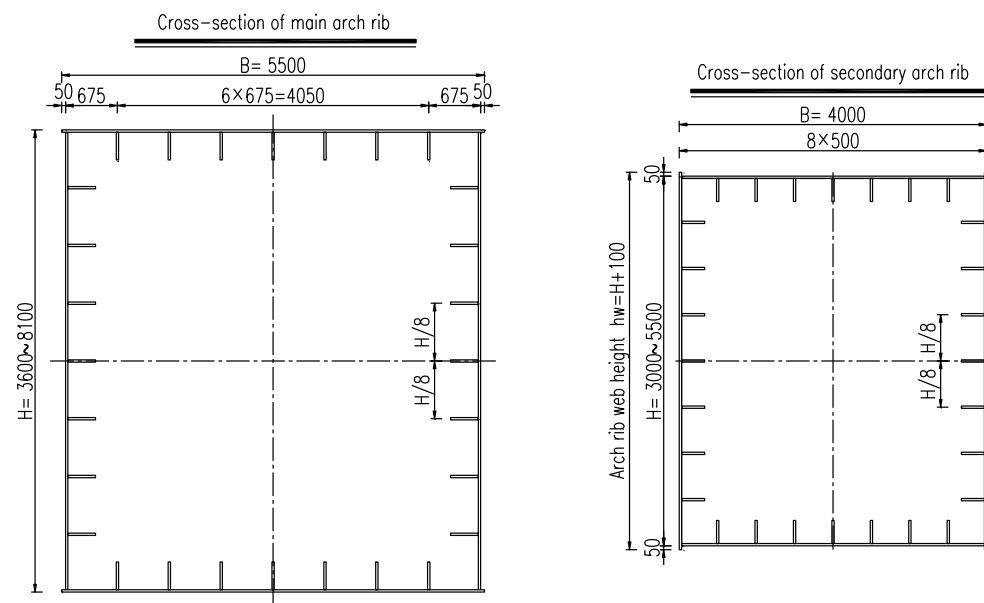


Figure 7 Variable cross section of the main arch rib (Unit: mm)

### 3.1.2 Secondary Arch

The main bridge has a secondary arch on both main spans. The secondary arch on the southern main span is located on the west side of the bridge deck, whereas the secondary arch on the northern main span is located on the east side. The two secondary arches are connected at the central arch feet by a transverse beam beneath the main beam, and at the side arch feet, they are connected to the main arch via transverse beams at the ends of the main arch ribs beneath the main beam. The two secondary arches have the same structure and are antisymmetric about the center point of the main bridge.

The plane of the secondary arch ribs is laterally outwardly inclined at an angle of  $25^\circ$ , with a span of 110 m and a distance of 30.0 m from the arch crown to the bridge deck. The main segment of the arch axis is a parabola, with a rise of 30 m and a span of 94 m, resulting in a rise-to-span ratio of 1/3.1. The connection between the arch feet and the transverse beam uses a circular arc with a radius of 10 m ( $R=10 \text{ m}$ ). A straight-line transition is used between the parabolic and circular arc segments. The cross section of the secondary arch ribs is rectangular. The parabolic segment of the arch ribs has a variable cross section, with dimensions of  $B \times H = 5.5 \text{ m} \times 4.0 \text{ m}$  where it transitions to the straight segment, and dimensions of  $B \times H = 3.0 \text{ m} \times 4.0 \text{ m}$  at the vertex of the parabola, with linear variation between them.

### 3.1.3 Spatial Bending–Twisting Surface at the Arch Feet

The connection transition structure between the main arch, secondary arch, and transverse beams (the arch foot twisting segment) is crucial for the unique landscape feature of the bridge and the force transfer between the main and secondary arches. The main and secondary arch feet are components with bending–twisting surfaces. Because the forces are complex, Q370qD steel is used in the design, with a plate thickness of 40 mm.

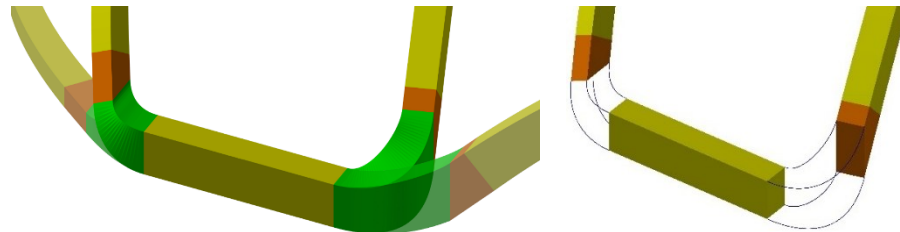


**Figure 8** Schematic of arch foot segment connection with a transverse beam

The shape of the arch foot segment is determined on the basis of the edge line of the arch rib as the reference. For the main arch, at the arch foot transition segment, the top and bottom plates of the arch rib are converted into the top and bottom plates of the transverse beam. For the secondary arch, at the arch foot transition segment, the top and bottom plates are converted into the web of the transverse beam, minimizing the number of bending–twisting surfaces to ensure smoother force transmission (see Figure 8). The arrangement of the diaphragms is optimized, with the intersection points of the diaphragms and edge lines determined on the basis of the length of the edge line. BIM software is used for the spatial layout of the diaphragms (see Figure 9) to ensure adequate space for processing operations and welding quality. The final goal is to achieve a smooth and aesthetically pleasing external shape for the arch foot, convenient and feasible processing and manufacturing, and a structurally coherent and rational force transmission system.

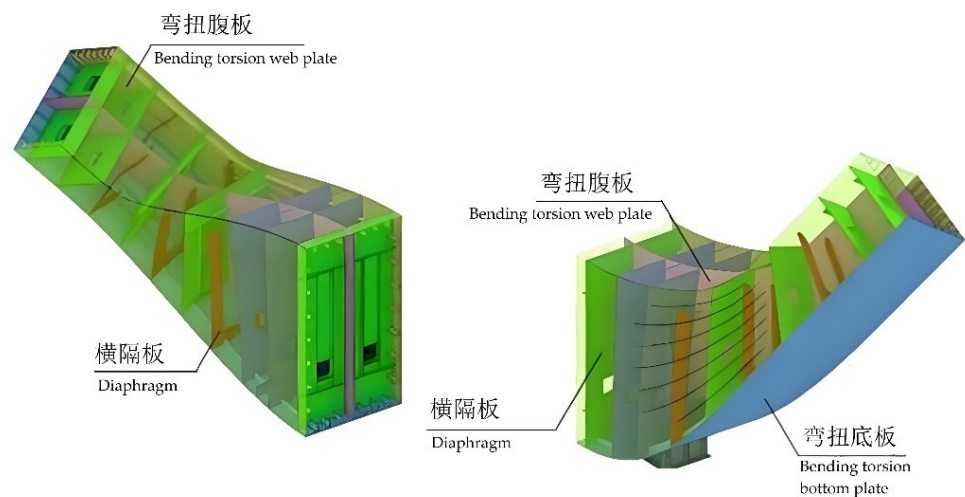


**Figure 9** Schematic of the arch foot diaphragm arrangement

### 3.1.4 Anchorage Structure on the Arch Rib

The main and secondary arches are connected to the hanging rods by lifting lugs. These lifting lugs are formed by extending partitions from the bottom plate locally (see Figure 10). The theoretical anchorage point on the arch is located 420 mm below the bottom plate of the arch rib.

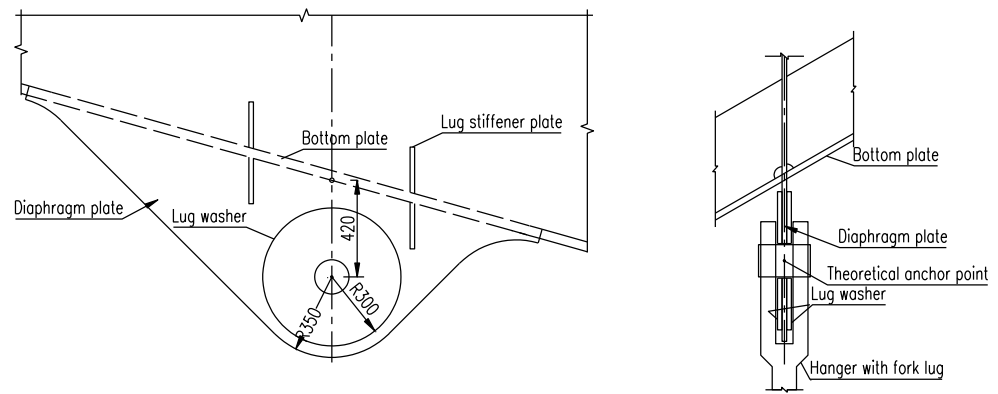


**Figure 10** Anchorage structure on the arch rib (Unit: mm)

### 3.2 Main Beam

The main beam adopted a semiclosed double-sided steel box cross section. The height between the top and bottom plates at the standard segment along the centerline is 4.0 m, and the standard segment width is 44.5 m (see Figure 11). The width of a single box is 8.7 m, with a cantilever length of 7.55 m, and the clear distance between the two box chambers is 12.0 m. The main beam is connected to the arch ribs through large transverse beams at the transverse beam locations. Two supports are set under the large transverse beam, with the centerlines of the supports located 22.5 m (main arch side) and 20 m (secondary arch side) from the bridge centerline. The main beam also has two supports at the auxiliary piers, with a support spacing of 22.9 m.

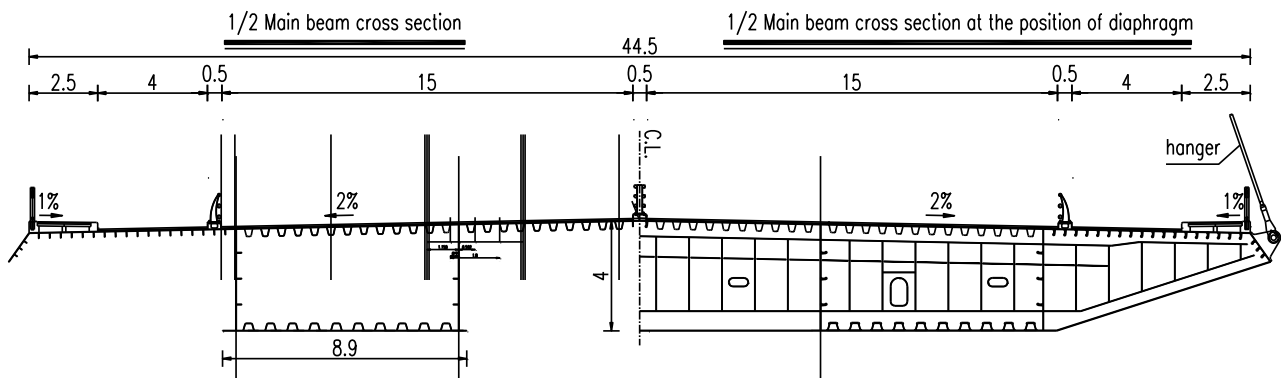


**Figure 11** Standard cross-section of the main beam (Unit: m)

The main beam is divided into 33 segments, each with a standard length of 12 meters. The thickness of the top, bottom, and web plates in the standard beam segment is 16 mm. In the negative bending moment zone of the central piers, the thickness of the top plate is locally increased to 24 mm, the bottom plate is increased to 40 mm, and the web plates are increased to 24 mm. The transverse diaphragms comprise cantilever web plates on both sides, two internal diaphragms within the box, and box separators, forming a solid web transverse diaphragm with a standard spacing of 3 m. The thickness of the diaphragm is 12 mm in general, 16 mm at the hanging rod positions, and 40 mm at the support positions.

The main beam is connected to the hanging rods by lifting lugs, which are integrated with the cantilever web plates of the box beam (see Figure 12). These lugs are formed by extending the cantilever web plates outward. The cantilever web plates are welded to the main beam's web plates, with welding positions inside the box and at the intervals between partitions, ensuring that the dead load and live load of the main beam can be smoothly transferred from the main beam through the hanging rods to the arch ribs.

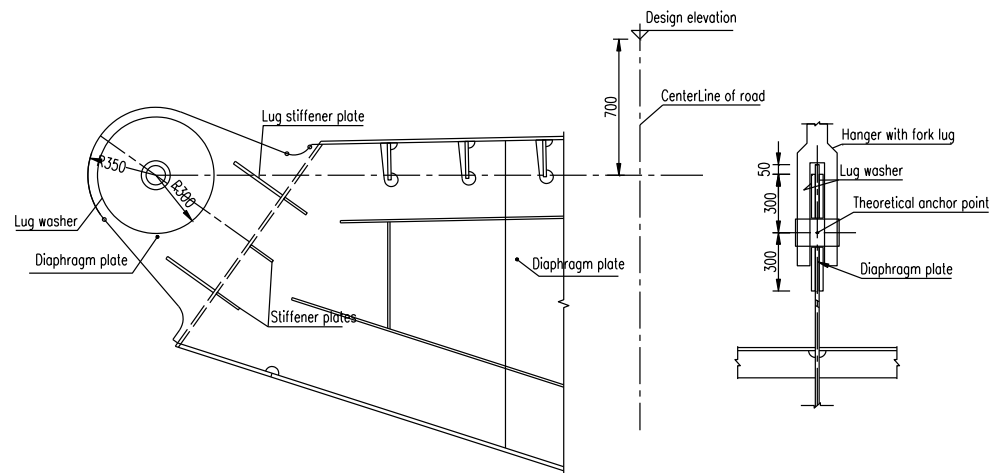


**Figure 12** Anchorage structure on the beam (Unit: mm)

### 3.3 Hanging Rod

The main bridge has 56 hanging rods (4×14), with the longest rod measuring 56 m. The rods use galvanized parallel steel wire ropes with a standard strength of 1670 MPa, and the specifications are PES7-73 and PES7-121. A 6-m spacing exists between the hanging rods on the beam and along the arch in the bridge direction. Owing to the diagonal span of the main arch and the outward inclination of the secondary arch, the hanging rods are arranged in a spatial twisting surface layout across the entire bridge. The hanging rods are anchored via a fork lug anchored at the beam and arch locations. To ensure structural collaboration between the arch and beam, the corresponding hanging rods in the longitudinal and transverse directions are synchronously and symmetrically tensioned.

### 3.4 Deck Pavement

The main bridge deck pavement uses cast-in-place asphalt concrete. The upper layer comprises 45-mm thick modified asphalt mastic stone (SMA-13), with a modified emulsified asphalt adhesive layer. The lower layer is a 35-mm thick layer of cast-in-place asphalt concrete (GA-10) [3], with a surface coating of premixed asphalt gravel with a particle size of 10–15 mm. The waterproof bonding layer uses MMA (methyl methacrylate resin).

### 3.5 Bearing and the Curved Surface Adjustment Structure

#### 3.5.1 Bearings

After detailed seismic analysis and a specialized comparative study, it was decided that the main bridge would adopt a seismic isolation system. Double-curvature spherical seismic isolation bearings are used to solve the issue of excessive longitudinal and transverse seismic forces on the bridge under an 8-degree earthquake. The isolation bearings are installed on top of the main pier and the bent cap of the approach bridge. The main arch foot bearing has a bearing capacity of 6000 tons; the secondary arch foot near the middle pier, 4000 tons; and the arch foot near the side span, 3500 tons.

#### 3.5.2 Steel-UHPC Composite Large-Tonnage Bearing Curved Adjustment Structure

To solve the adjustment issue of the bearings under the twisted arch foot structure, a steel-UHPC composite large-tonnage bearing curved adjustment structure is used. This structure provides adjustment functionality for the bearings at the arch foot. The adjustment structure comprises six steel plates arranged in a cross pattern (see Figure 13), which resolves the slope problem caused by the spatial curved surface. While ensuring that the steel plates in the adjustment structure can bear the required load and considering the durability and reliability of the structure, UHPC (Ultra-High Performance Concrete) is poured into the adjustment components to



form a steel-UHPC composite structure. This approach converts line pressure into surface pressure, enhancing the overall integrity of the structure. Additionally, air is expelled from the structure to prevent the risk of steel corrosion.

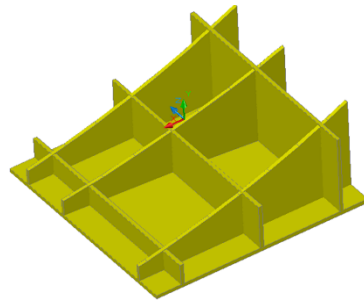


Figure 13 Adjustment structure diagram

### 3.6 Substructure

The main bridge pier is a four-sided truncated pyramid with upper dimensions of 7 m × 5.4 m, lower dimensions of 10 m × 10 m, and a pier height of 6.9 m. The cap foundation has dimensions of 18 m × 18 m and a thickness of 4 m, supported by 3×3 = 9 drilled grouting piles with a diameter of 2.5 m. The cap foundations are connected by a tie beam, which has the same thickness as the cap foundation and a width of 8 m. Below this tie beam are two drilled grouting piles with a diameter of 2.5 m (see Figure 14).

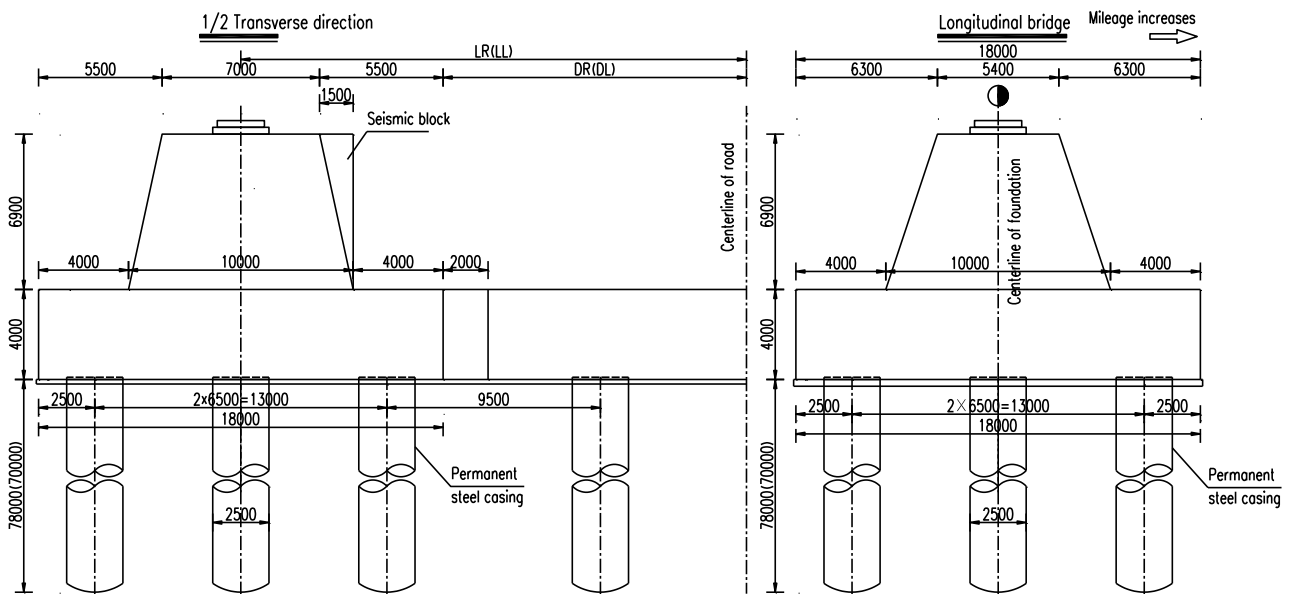


Figure 14 Main pier structure (Unit: mm)

The main bridge is located in a high-seismic-intensity zone, and the seismic design adopts a seismic isolation system to reduce the foundation's force under seismic conditions. Owing to the presence of a certain thickness of fine sand and silty sand layers at the site, permanent load-bearing steel casings with a wall thickness of 20 mm are used for the bridge's pile foundations to ensure structural safety.

## 4 Bridge Structural Analysis

### 4.1 Main Bridge Overall Structural Analysis

The Midas Civil finite element program is used to establish a spatial analysis model for the main beam and arch ribs and performs a comprehensive analysis of the static, fatigue, stability, and seismic performance of the entire bridge.

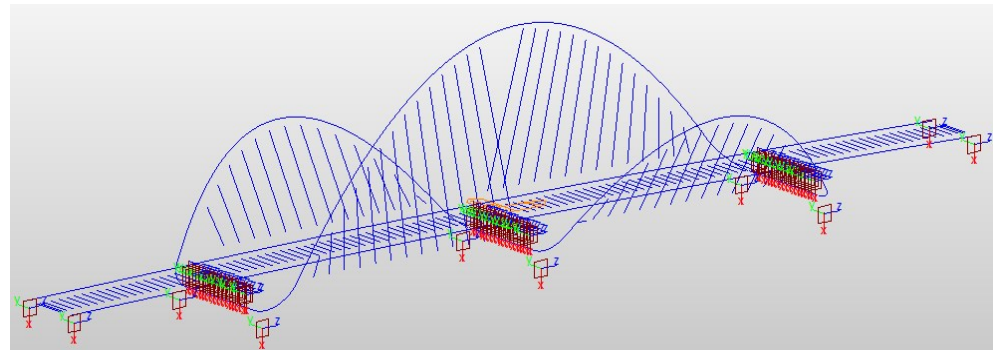


**Figure 15** Spatial finite element model of the main bridge

The calculation results are as follows:

- (1) **Static Strength:** The shear lag effect should be considered for the steel structure main beam, and an effective section reduction should be applied. Additionally, the influence of local stability should be considered when calculating and controlling the stress. The shear stress control values are determined on the basis of the plate thickness, referring to the relevant specifications. For the main beam under the basic load combinations, the maximum tensile and compressive stresses at the top of the main beam are 205 MPa and 74 MPa, respectively (see Figure 17), whereas the maximum tensile and compressive stresses at the bottom are 178 MPa, all of which are less than 270 MPa (the material's strength). The maximum positive and negative shear stresses are 102 MPa and 103 MPa, respectively, which are less than 155 MPa (the shear strength of the material). For the arch ribs under basic load combinations, the maximum tensile and compressive stresses are 196 MPa and 91 MPa, respectively (see Figure 18), which are below 270 MPa; the maximum shear stress is 51 MPa, which is below 150 MPa. All values meet the code requirements.

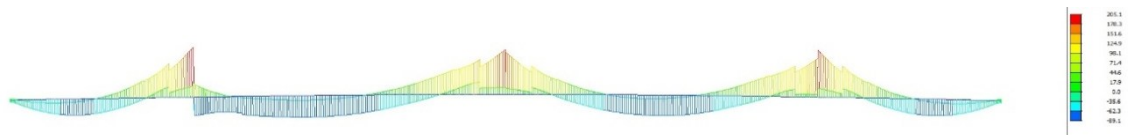


**Figure 16** Stress envelope of the upper edge of the main beam under the basic load combination (Unit: MPa)

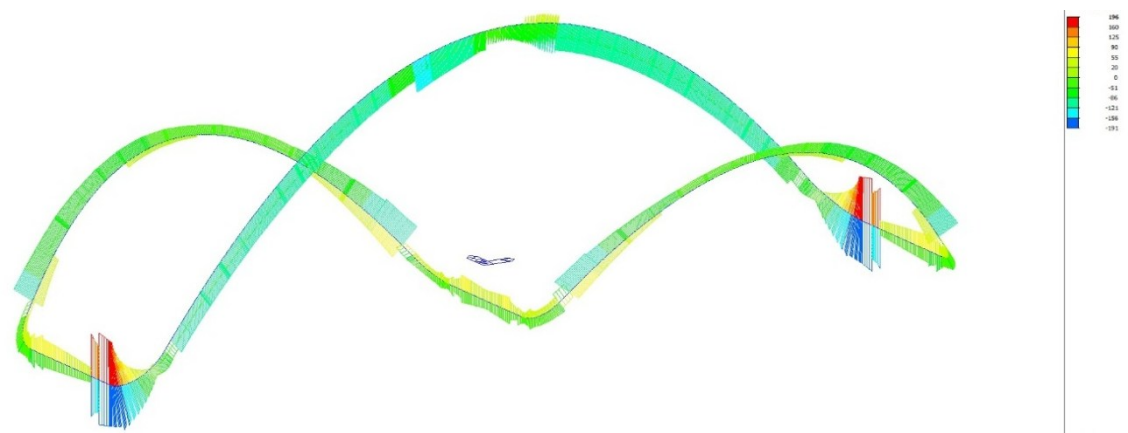


**Figure 17** Stress envelopes of arch ribs under the basic load combination (Unit: MPa)

- (2) **Static Stiffness:** The live load deflection of the main beam is  $40 + 16 = 56$  mm, which is less than  $110 \text{ m}/500 = 220$  mm. The live load deflection of the main arch is  $28 + 19 = 46$  mm, which is less than  $220 \text{ m}/1000 = 220$  mm. The live load

deflection of the secondary arch is  $9 + 6 = 15$  mm, which is less than  $110 \text{ m}/1000 = 110$  mm. All values meet the code requirements.

- (3) **Fatigue Strength:** In the fatigue test, the calculation model is consistent with the static strength calculation model. Vehicle loads are applied according to the fatigue load calculation Model I, with a primary focus on the longitudinal fatigue stress amplitude of the main beam and the fatigue stress amplitude of the hanging rods. On the basis of fatigue details [4], the fatigue stress amplitude limits for the base material and primary welds of the main beam and arch ribs are determined to be 76 MPa and 68 MPa, respectively, whereas the fatigue stress amplitude limit for the hanging rods is 102 MPa. These values are greater than the fatigue stress amplitudes for the main beam, arch ribs, and hanging rods calculated via fatigue load Model I, thus meeting the code requirements.
- (4) **Overall Stability:** The overall elastic stability coefficient of the arch ribs is 24.01, with the instability mode being out-of-plane buckling. This stability coefficient meets the code requirement.
- (5) **Dynamic Characteristics:** The first five modes of the bridge and corresponding natural frequencies are as follows: First mode: 0.662 Hz, transverse bending of the main arch in a diagonal span. Second mode: 0.807 Hz, antisymmetric vertical bending of the main beam. Third mode: 1.143 Hz, vertical bending of the main arch in a diagonal span. Fourth mode: 1.261 Hz, antisymmetric transverse bending of the main arch in a diagonal span. Fifth mode: 1.393 Hz, transverse bending of the outward-inclined secondary arch.
- (6) **Seismic Performance:** Nonlinear time history analysis is used to calculate the seismic response of the entire bridge, considering the impact of adjacent approach bridges on the main bridge's seismic response. The seismic response under the seismic isolation system is computed, and foundation checks are performed. The allowable bearing capacity and cross-sectional strength of the pile foundation are controlled by seismic forces. The existing pile foundation length and reinforcement meet the code requirements.

#### 4.2 Local Analysis of the Arch Foot

The main arch foot, the side arch foot of the secondary arches, and the middle arch foot of the secondary arches experience three-dimensional torsion; thus, the buckling conditions of these corresponding parts must be analyzed. Among them, the main arch foot is the most critical in terms of stress, so this section only briefly presents the local analysis results of the main arch foot.

The Ansys finite element program was used to establish a full-bridge global-local hybrid model for three-dimensional solid analysis of the main arch foot of the bridge. In the local model, the arch foot is represented via 'Shell 43' elements, whereas in the global model, elements such as the main beam, arch ribs, and transverse beams are represented via 'Beam 4' elements. The local model is connected to the global model via rigid domain connections. The solid modeling section starts from the initial bending point outside the main arch axis and extends to the junction between the arch box and the transverse beams. The model accurately reproduces the locations of the internal diaphragms, stiffeners, and openings within the actual arch foot and reflects the actual plate thicknesses of each component. The external contour of the main arch foot solid model is shown in Figure 18.

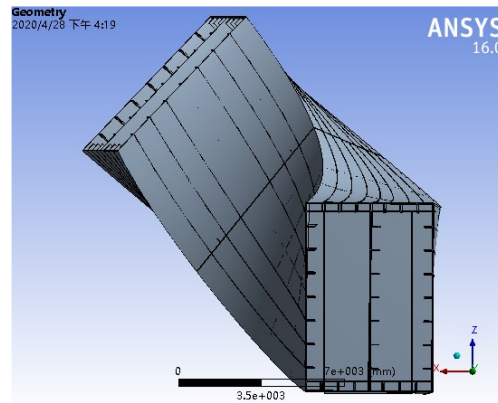


**Figure 18** Main arch foot solid finite element model

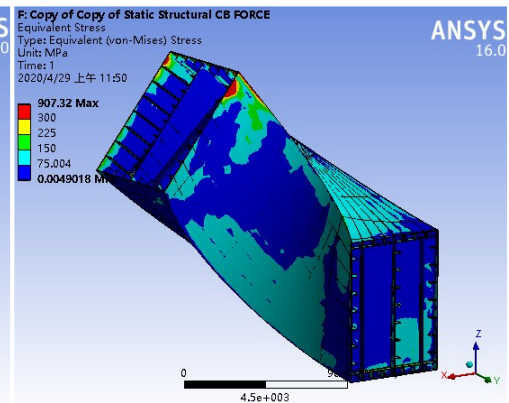


**Figure 19** Stress distribution diagram of the arch foot

The calculation results show that the inner surface of the main arch foot is under tension, whereas the outer surface is under compression. The Von-Mises stress in the internal diaphragms, stiffening ribs, and other structural components of the arch foot can mostly be controlled below 100 MPa. The Von-Mises stress on the four external surfaces of the arch foot can mostly be controlled below 150 MPa, as shown in Figure 19.

### 5 Conclusions

The Xiaohe River Bridge on Dayun Road innovatively adopted a spatial anti-symmetric spiral-shaped ribbon-arch bridge for the first time in China. This bridge features a novel structural form and an aesthetically pleasing design. The main bridge comprises a single large diagonal main arch, two outward-inclined secondary arches, and connecting transverse beams that together form a spiral-shaped ribbon-arch rib, which combines with semienclosed bilateral steel box girders to create an arch-beam composite system. The main bridge is a self-balancing structure without external thrust. The main and secondary arches use steel box cross sections with parabolic arch axis lines, and the arch footings are constructed using ultra-thick plates with spatially twisted surfaces. At the bearing positions, large-capacity steel-UHPC (Ultra-High Performance Concrete) composite bearings with curved surface adjustment structures are employed.

The bridge uses a double-curved spherical seismic isolation bearing system, and the foundation is supported by drilled grouting piles. The results of the global and local structural calculations indicate that the bridge exhibits excellent mechanical performance, ensuring safety and reliability, all of which meet design codes and standards. The design and analytical methods employed are groundbreaking and could serve as a reference for future similar projects. Construction of the bridge began in June 2019 and was completed and accepted in January 2022.

**Conflict of interest:** All the authors disclosed no relevant relationships.

**Data availability statement:** The data that support the findings of this study are available from the corresponding author, Teng, upon reasonable request.

### References

1. Zhao, J.; Wan, J.; Wen, J. Research on Aesthetics and Mechanical Performance of Dayun Road Bridge in Comprehensive Reform Zone of Shanxi Province. *World Bridges* **2022**, *50*, 7-12, doi:10.3969/j.issn.1671-7767.2022.01.002.
2. Tongji Architectural Design (Group) Co., L., . The Drawings of Xiaohe River Bridge on Dayun Road. **2019**.

3. Hu, H.; Zhao, J.; Ren, Y.; An, L.; Liu, Y. Overall Design of Main Bridge of Mingzhu Bay Bridge in Guangzhou. *Bridge Construction* **2021**, *51*, 93-99, doi:10.3969/j.issn.1003-4722.2021.03.013.
4. Ministry of Transport of the People's Republic of China JTG D64—2015 Specification for Design of Highway Steel Bridge. China Communications Press: Beijing, 2015.

#### AUTHOR BIOGRAPHIES



**Xiaozhu Teng**

M.E., Senior Engineer. Working at Tongji Architectural Design (Group) Co., Ltd.

Research Direction: Bridge engineering design and research.

Email: bamboo389@126.com